

# Modeling Nonconvex Constraints Using Linear Complementarity

Kevin Egan

Department of Computer Science  
Rensselaer Polytechnic Institute  
Troy, NY 12180  
Email: ktegan@cs.rpi.edu

Stephen Berard

Department of Computer Science  
Rensselaer Polytechnic Institute  
Troy, NY 12180  
Email: sberard@cs.rpi.edu

J.C. Trinkle

Department of Computer Science  
Rensselaer Polytechnic Institute  
Troy, NY 12180  
Email: trink@cs.rpi.edu

**Abstract**—Many physical simulators linearize contact constraints such that each contact constraint defines a half-space in the configuration space of the effected objects. By modeling contact constraints as infinitely extending half spaces it is only possible to approximate regions in configuration space that are locally convex. This implicit assumption of local convexity introduces artifacts in the results of the simulation. We present a new method for modeling regions of configuration space that are locally nonconvex using a linear complementarity formulation. From this we show that we can now accurately represent any general polytope using linear complementarity.

## I. INTRODUCTION

The linear complementarity problem, or LCP, was first used by Lötstedt [1] to formulate multi-body unilateral contact problems. Further work on linear and non-linear complementarity methods for multi-body contact were developed by Baraff [2] and Pfeiffer [3]. Both of these methods compute the instantaneous acceleration and velocity for a system of objects in contact. Most formulations linearize the contact constraints, treating all contact surfaces as planar, although some non-linear methods have worked with curved surfaces [4]. When using an instantaneous analysis, interpenetration between bodies may occur after the velocities are integrated forward by a finite time step.

The linear time-stepping method introduced by Stewart and Trinkle [5] integrates velocities and positions forward in time in such a manner that the linearized contact constraints are satisfied at the end of each time step. In the Stewart-Trinkle time stepping approach each contact surface is linearized to reduce the interpenetration constraint to a half-space constraint in configuration space, (also called C-space). This leads to erroneous or incorrect collisions occurring when objects move towards sharp corners. Because the LCP formulation requires that each and every contact constraint is satisfied, the valid region for a single object is defined as the intersection of some number of half-spaces in C-space. The intersection of many convex sets is itself a convex set, therefore the straight forward LCP formulation treats all contact constraints as convex regions in C-space. In this paper we show ways to modify the Stewart-Trinkle LCP formulation of the dynamic model to include nonconvex constraints.

We have found that the new techniques presented in this paper were fairly easy to incorporate into our existing LCP

based simulation. Furthermore, the novel techniques presented in this paper immediately corrected simulation inaccuracies caused by the implicit assumption of local convexity, as can be seen in Fig. 1.

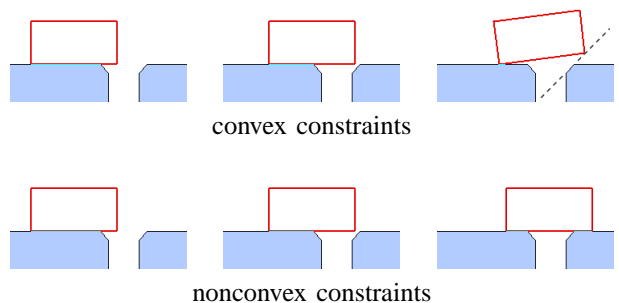


Fig. 1. The above screenshots were taken from a matlab program simulating a block sliding over a hole. In both examples there is a potential contact with the lower right corner of the block and the diagonal edge of the right side of the hole. If the C-space of the block can only use convex constraints then the diagonal edge on the right side of the hole is incorrectly modeled as extending forever. Using nonconvex constraints the block correctly slides past the corner.

## II. DYNAMIC MODEL

A linear complementarity problem (LCP) is defined as follows [6]: Given a constant matrix  $\mathbf{B} \in \mathbb{R}^{m \times m}$  and constant vector  $\mathbf{b} \in \mathbb{R}^m$ , find vectors  $\mathbf{z} \in \mathbb{R}^m$  and  $\mathbf{y} \in \mathbb{R}^m$  satisfying the following conditions:

$$\mathbf{y} = \mathbf{B}\mathbf{z} + \mathbf{b}, \quad (1)$$

$$0 \leq \mathbf{y} \perp \mathbf{z} \geq 0, \quad (2)$$

where  $\mathbf{y} \perp \mathbf{z}$  is the perpendicularity constraint  $\mathbf{y}^T \mathbf{z} = 0$ .

The time-stepping method formulates the linearized dynamics problem as the following [5]:

$$\mathbf{M}(\boldsymbol{\nu}^{l+1} - \boldsymbol{\nu}^l) = \mathbf{W}_n \mathbf{p}_n^{l+1} + \mathbf{W}_f \mathbf{p}_f^{l+1} + \mathbf{p}_{ext}^l, \quad (3)$$

$$\mathbf{q}^{l+1} - \mathbf{q}^l = h\mathbf{G}(\mathbf{q}^l)\boldsymbol{\nu}^{l+1}. \quad (4)$$

The unknown vector  $\boldsymbol{\nu}^{l+1}$  represents generalized velocity at the end of the current time step  $[t_l, t_{l+1}]$ . Similarly the unknown vector  $\mathbf{q}^{l+1}$  represents generalized position at time  $t_{l+1}$ . The time step duration is represented by  $h$ . The unknown vectors  $\mathbf{p}_n^{l+1}$  and  $\mathbf{p}_f^{l+1}$  represent the magnitude of impulses

applied during the current time step in the normal and tangential direction respectively. The vector  $\mathbf{p}_{ext}^l$  represents the magnitude of all external impulses. The matrices  $\mathbf{W}_n$  and  $\mathbf{W}_f$  are Jacobian or “wrench” matrices that map contact forces to wrenches in the body-fixed frame. The matrix  $\mathbf{G}(\mathbf{q})$  is a Jacobian matrix that maps the object velocity  $\boldsymbol{\nu}$  to the rate of change for object configuration  $\mathbf{q}$ .

The complementarity formulation becomes the following [5]:

$$0 \leq \mathbf{y} = \begin{bmatrix} \mathbf{W}_n^T \boldsymbol{\nu}^{l+1} + \mathbf{f}^l/h \\ \mathbf{W}_f^T \boldsymbol{\nu}^{l+1} + \mathbf{E} \mathbf{s}^{l+1} \\ \mathbf{U} \mathbf{p}_n^{l+1} - \mathbf{E}^T \mathbf{p}_f^{l+1} \end{bmatrix} \perp \begin{bmatrix} \mathbf{p}_n^{l+1} \\ \mathbf{p}_f^{l+1} \\ \mathbf{s}^{l+1} \end{bmatrix} = \mathbf{z} \geq 0. \quad (5)$$

The first and third rows in Eqn. (5) contain vectors that represent  $n$  constraints for  $n$  contacts. The second row represents  $kn$  constraints where  $k$  is the number of spanning vectors used to approximate the friction cone [5]. The matrix  $\mathbf{E} \in \mathbb{R}^{kn \times n}$  is block diagonal with nonzero blocks given by  $[1, 1, \dots, 1]^T \in \mathbb{R}^k$ . The diagonal matrix  $\mathbf{U}$  stores friction coefficients. The vector  $\mathbf{f}^l$  contains distances to each current and potential contact. The  $\mathbf{f}^l/h$  term is a constraint stabilization term. The unknown vector  $\mathbf{s}^{l+1}$  is a scaling factor for the tangential impulses in the unknown vector  $\mathbf{p}_f^{l+1}$ . By solving Eqn. (3) for  $\boldsymbol{\nu}^{l+1}$  in terms of  $\mathbf{p}_n^{l+1}$ ,  $\mathbf{p}_f^{l+1}$  and  $\mathbf{s}^{l+1}$  we can obtain the following values for  $\mathbf{B}$  and  $\mathbf{b}$  introduced in Eqn. (1):

$$\mathbf{B} = \begin{bmatrix} \mathbf{W}_n^T \mathbf{M}^{-1} \mathbf{W}_n & \mathbf{W}_n^T \mathbf{M}^{-1} \mathbf{W}_f & 0 \\ \mathbf{W}_f^T \mathbf{M}^{-1} \mathbf{W}_n & \mathbf{W}_f^T \mathbf{M}^{-1} \mathbf{W}_f & \mathbf{E} \\ \mathbf{U} & -\mathbf{E}^T & 0 \end{bmatrix}, \quad (6)$$

$$\mathbf{b} = \begin{bmatrix} \mathbf{W}_n^T (\boldsymbol{\nu}^l + \mathbf{M}^{-1} \mathbf{p}_{ext}) + \mathbf{f}^l/h \\ \mathbf{W}_f^T (\boldsymbol{\nu}^l + \mathbf{M}^{-1} \mathbf{p}_{ext}) \\ 0 \end{bmatrix}. \quad (7)$$

Equations (6) and (7) give the complete LCP formulation when using convex constraints. We can now solve for  $\mathbf{z}$  which contains  $\mathbf{p}_n^{l+1}$ ,  $\mathbf{p}_f^{l+1}$  and  $\mathbf{s}^{l+1}$ . We then use these values to compute  $\boldsymbol{\nu}^{l+1}$  and  $\mathbf{q}^{l+1}$ .

### III. NON-PENETRATION CONSTRAINT

In this section we focus on the non-penetration constraint for the case of a point mass approaching with two potential contacts. For a point mass, C-space and physical space are identical.

$$0 \leq \mathbf{W}_{1n}^T \boldsymbol{\nu}^{l+1} + f_1^l/h \perp p_{1n}^{l+1} \geq 0, \quad (8)$$

$$0 \leq \mathbf{W}_{2n}^T \boldsymbol{\nu}^{l+1} + f_2^l/h \perp p_{2n}^{l+1} \geq 0. \quad (9)$$

This formulation can accurately model convex features in C-space such as in Fig. 2(a) where we see a point mass approaching a corner with convex constraints. In Fig. 2(b) we see a point mass approaching a corner with nonconvex constraints. Simulations that use the convex formulation will mistakenly model all corners as having convex constraints.

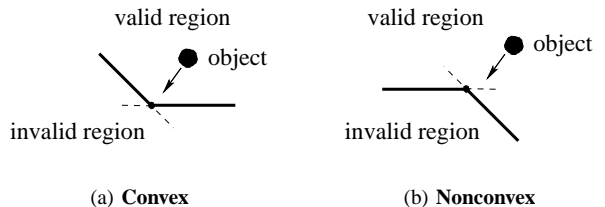


Fig. 2. The convex feature on the left allows the intersection of the valid regions for the two planes. The nonconvex feature on the right allows the union of the valid regions for the two planes.

**Problem 1:** Model the valid region in C-space as the union of two half-spaces, instead of the intersection of two half-spaces. All other physical properties should remain unchanged from the convex formulation.

The penetration gap at the end of the current time step divided by  $h$  is calculated in the left side of Eqns. (8) and (9). We temporarily ignore friction and external forces and define this value for each plane as  $a_1$  and  $a_2$ :

$$a_1 = \mathbf{W}_{1n}^T (\boldsymbol{\nu}^l + \mathbf{M}^{-1} (\mathbf{W}_{1n} \mathbf{p}_{1n}^{l+1} + \mathbf{W}_{2n} \mathbf{p}_{2n}^{l+1})) + f_1^l/h, \quad (10)$$

$$a_2 = \mathbf{W}_{2n}^T (\boldsymbol{\nu}^l + \mathbf{M}^{-1} (\mathbf{W}_{1n} \mathbf{p}_{1n}^{l+1} + \mathbf{W}_{2n} \mathbf{p}_{2n}^{l+1})) + f_2^l/h. \quad (11)$$

An object will lie in the union of two contact constraint half-spaces if either  $a_1 \geq 0$  or  $a_2 \geq 0$ . Modeling this “or” relationship is not straightforward because the LCP formulation requires that each and every constraint is satisfied. It is not possible to specify a logical “or” relationship such that only one of two constraints must be satisfied. Therefore, we propose two new LCP formulations to solve this problem. The “max” formulation maintains more physical accuracy but requires more constraints, whereas the “summation” formulation is less physically accurate but can be expressed using fewer constraints.

### IV. MAX FORMULATION

The first “max” formulation depends on the following logical relation (we express logical or as  $\vee$ , logical and as  $\wedge$ , and logical equivalence as  $\iff$ ):

$$(a_1 \geq 0) \vee (a_2 \geq 0) \iff \max\{a_1, a_2\} \geq 0. \quad (12)$$

**Proposition 1:** The following LCP based on the max formulation assures that the valid region is the union of two half-spaces. It also assures that contact force is generated only for planes in contact.

Based on Eqn. (12), we enforce constraints on the expressions  $a_1$  and  $a_2$ . For now we will ignore friction and external forces, so that the  $a_1$  and  $a_2$  expressions are each linear in the unknowns  $p_{1n}^{l+1}$  and  $p_{2n}^{l+1}$ , as seen in Eqns. (10) and (11). Artificial variables  $c_1, c_2, d, g_1, g_2, h_1, h_2$  and  $p$  are created. Additionally, a large positive constant  $\gamma$  is used. The following

equations are meant to replace Eqns. (8) and (9) when it is necessary to model a nonconvex feature in C-space:

$$0 \leq c_1 + a_1 - 1 \perp c_1 \geq 0 \quad (13)$$

$$0 \leq c_2 + a_2 - 1 \perp c_2 \geq 0 \quad (14)$$

$$0 \leq g_1 + g_2 - 1 \perp d \geq 0 \quad (15)$$

$$0 \leq c_1 + d - \gamma \perp g_1 \geq 0 \quad (16)$$

$$0 \leq c_2 + d - \gamma \perp g_2 \geq 0 \quad (17)$$

$$0 \leq h_1 + a_1 \perp h_1 \geq 0 \quad (18)$$

$$0 \leq h_2 + a_2 \perp h_2 \geq 0 \quad (19)$$

$$0 \leq d - \gamma + 1 \perp p \geq 0 \quad (20)$$

$$0 \leq h_1 + d - \gamma + 1 \perp p_{1n}^{l+1} \geq 0 \quad (21)$$

$$0 \leq h_2 + d - \gamma + 1 \perp p_{2n}^{l+1} \geq 0. \quad (22)$$

Eqns. (13) and (14) constrain  $c_1 = |\min\{a_1, 1\} - 1|$  and  $c_2 = |\min\{a_2, 1\} - 1|$ . Eqns. (18) and (19) constrain  $h_1 = |\min\{a_1, 0\}|$  and  $h_2 = |\min\{a_2, 0\}|$ . Eqns. (15), (16) and (17) are designed to find the maximum value of  $a_1$  and  $a_2$ .

As long as  $\gamma > \max\{c_1, c_2\}$  we will have  $d > 0$  from Eqns. (13), (14), (16) and (17). In general  $d \geq \max\{\gamma - c_1, \gamma - c_2\}$ . Because  $d > 0$  the third equation forces  $g_1 + g_2 = 1$ , and therefore  $g_1 > 0$  or  $g_2 > 0$ . To make  $g_1$  or  $g_2$  greater than 0 either  $d + c_1 - \gamma = 0$  or  $d + c_2 - \gamma = 0$ . This fixes  $d$  to either  $\gamma - c_1$  or  $\gamma - c_2$ , which in turn implies a strict equality  $d = \max\{\gamma - c_1, \gamma - c_2\}$ . We have manipulated  $d$  to select the smaller of the  $c_1$  and  $c_2$  values, and therefore select the maximum (least negative) of  $a_1$  and  $a_2$ . Relating  $d$  to  $a_1$  and  $a_2$ , we can say  $d = \min\{\max\{a_1, a_2\}, 1\} + \gamma - 1$ . Finally we have  $d - \gamma + 1 = \min\{\max\{a_1, a_2\}, 1\}$ . In the degenerate case where  $c_1 = c_2$  both  $g_1$  and  $g_2$  may be greater than 0, but this does not change the relationship between  $d$ ,  $a_1$  and  $a_2$ .

Notice that  $d - \gamma + 1$  is equivalent to the right side of Eqn. (12) except for an extra min term. The min term is not important for our purposes since  $\min\{\max\{a_1, a_2\}, 1\} \geq 0$  implies that  $\max\{a_1, a_2\} \geq 0$ , which is what we are really interested in. If  $d - \gamma + 1 > 0$  we have no contact, and if  $d - \gamma + 1 = 0$  we do have contact.

In Eqn. (20) we have  $d - \gamma + 1 \geq 0$  which enforces the non-penetration constraint. Note that  $p$  in Eqn. (20) is not used in any other equation, and has no effect on the formulation. In Eqns. (21) and (22), the normal force magnitude for individual planes of the nonconvex constraint are calculated. For  $p_{1n}^{l+1}$  to be greater than 0, both  $d - \gamma + 1$  and  $h_1$  must be 0. This enforces the rule that a contact force can only come from a plane that is in contact.

To make the formulation work, the constant value  $\gamma$  must be greater than  $|\min\{a_1, a_2, 0\}|$  to force  $d$  to be positive in Eqns. (16) and (17). To be conservative  $\gamma$  can be set to the diameter of the scene, or the twice the distance the fastest point can travel in the next time step.

Let us create two simple examples, one without contact as pictured in Fig. 3(a), and one with contact as pictured in Fig. 3(b). For both examples the point has mass 1, and the time

step  $h$  is set to 2. The only difference in the two examples is the current velocity  $\nu^l$ . In the first example  $\nu^l = [-2, 0]^T$ , and in the second example  $\nu^l = [-2, -1]^T$ . In these examples we set  $p_{1n}^{l+1}$  to represent the contact impulse along the vertical plane  $x = 0$ , and  $p_{2n}^{l+1}$  to represent the contact impulse along the horizontal plane  $y = 0$ . This sets  $a_1$  and  $a_2$  to represent penetration distance divided by time step in x and y respectively. Since each constraint is aligned with an axis and we have a time step of 2  $q^{l+1} = [2a_1, 2a_2]^T$

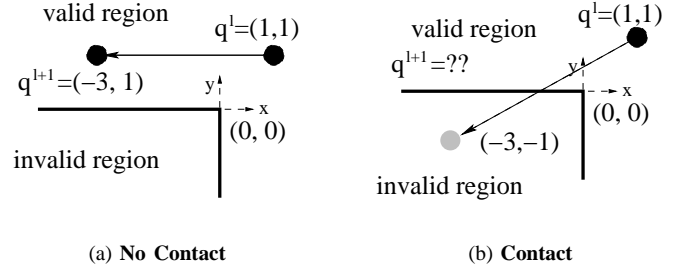


Fig. 3. In the left example no contact occurs, in the right example contact does occur. In the right example the point would reach  $q^{l+1} = [-3, -1]^T$  if no constraints were present, but since contact is made a different must be obtained.

We used an LCP solver to compute the unique frictionless solution  $z_a$  for the example in Fig. 3(a). There are three solutions for the example shown in 3(b): contact with both planes ( $z_{b1}$ ), contact with the vertical plane ( $z_{b2}$ ), and contact with the horizontal plane ( $z_{b3}$ ). We obtained  $z_{b1}$  from an LCP solver and found the other two solutions by hand. The example in Fig. 3(a) uses  $B_a$  and  $b_a$ , and the example in Fig. 3(b) uses  $B_b$  and  $b_b$ . For all solutions  $\gamma = 100$ .

In the example seen in Fig. 3(a) no contact occurs and the solution  $z_a$  dictates that the point mass has velocity  $\nu^{l+1} = [-2, 0]^T$ , position  $q^{l+1} = [-3, 1]^T$ , and  $a_1 = -1.5$ ,  $a_2 = 0.5$  at the end of the current time step.

For  $z_{b1}$ , the first solution to the example in Fig. 3(b), contact is made with both planes and contact impulses  $p_{1n}^{l+1} = 1.5$  and  $p_{2n}^{l+1} = 0.5$  are applied. In this solution the point mass has velocity  $\nu^{l+1} = [-0.5, -0.5]^T$  and position  $q^{l+1} = [0, 0]^T$  at the end of the current time step. The penetration distance divided by time step for both planes,  $a_1$ ,  $a_2$ , is 0 since there is contact with both planes. For  $z_{b2}$ , the second solution to the example in Fig. 3(b), contact only occurs with the vertical plane. In this solution we have  $a_1 = 0$ ,  $a_2 = -0.5$ ,  $p_{1n}^{l+1} = 1.5$ ,  $p_{2n}^{l+1} = 0$ ,  $\nu^{l+1} = [-0.5, -1]^T$  and position  $q^{l+1} = [0, -1]^T$ . For  $z_{b3}$ , the third solution to the example in Fig. 3(b), contact only occurs with the horizontal plane. In this solution we have  $a_1 = -1.5$ ,  $a_2 = 0$ ,  $p_{1n}^{l+1} = 0$ ,  $p_{2n}^{l+1} = 0.5$ ,  $\nu^{l+1} = [-2, -0.5]^T$  and position  $q^{l+1} = [-3, 0]^T$ .

$$B_a = B_b = \begin{bmatrix} 1 & 0 & 0 & 0 & 0 & 0 & 0 & 0 & 1 & 0 \\ 0 & 1 & 0 & 0 & 0 & 0 & 0 & 0 & 0 & 1 \\ 0 & 0 & 0 & 1 & 1 & 0 & 0 & 0 & 0 & 0 \\ 1 & 0 & 1 & 0 & 0 & 0 & 0 & 0 & 0 & 0 \\ 0 & 1 & 1 & 0 & 0 & 0 & 0 & 0 & 0 & 0 \\ 0 & 0 & 0 & 0 & 0 & 1 & 0 & 0 & 1 & 0 \\ 0 & 0 & 0 & 0 & 0 & 0 & 1 & 0 & 0 & 1 \\ 0 & 0 & 1 & 0 & 0 & 0 & 0 & 0 & 0 & 0 \\ 0 & 0 & 1 & 0 & 0 & 1 & 0 & 0 & 0 & 0 \\ 0 & 0 & 1 & 0 & 0 & 0 & 1 & 0 & 0 & 0 \end{bmatrix}$$

$$b_a = \begin{bmatrix} -2.5 \\ -0.5 \\ -1 \\ -100 \\ -100 \\ -1.5 \\ 0.5 \\ -99 \\ -99 \\ -99 \end{bmatrix} \quad b_b = \begin{bmatrix} -2.5 \\ -1.5 \\ -1 \\ -100 \\ -100 \\ -1.5 \\ -0.5 \\ -99 \\ -99 \\ -99 \end{bmatrix}$$

$$z_a = \begin{bmatrix} c_1 \\ c_2 \\ d \\ g_1 \\ g_2 \\ h_1 \\ h_2 \\ p \\ p_{1n}^{l+1} \\ p_{2n}^{l+1} \end{bmatrix} = \begin{bmatrix} 2.5 \\ 0.5 \\ 99.5 \\ 0 \\ 1 \\ 1.5 \\ 0 \\ 0 \\ 0 \\ 0 \end{bmatrix}$$

$$z_{b1} = \begin{bmatrix} 1 \\ 1 \\ 99 \\ 0 \\ 1 \\ 0 \\ 0 \\ 0 \\ 1.5 \\ 0.5 \end{bmatrix} \quad z_{b2} = \begin{bmatrix} 1 \\ 1.5 \\ 99 \\ 1 \\ 0 \\ 0 \\ 0.5 \\ 0 \\ 1.5 \\ 0 \end{bmatrix} \quad z_{b3} = \begin{bmatrix} 2.5 \\ 1 \\ 99 \\ 0 \\ 1 \\ 1.5 \\ 0 \\ 0 \\ 0 \\ 0.5 \end{bmatrix}$$

## V. SUMMATION FORMULATION

Our second nonconvex formulation is not as accurate, but it creates a smaller more efficient LCP. For the “summation” formulation we would like to use something close to the following logical relation:

$$(a_1 > 0) \vee (a_2 > 0) \iff \max\{0, a_1\} + \max\{0, a_2\} > 0. \quad (23)$$

Unfortunately, the logical relationship in Eqn. (23) does not hold true if the strict inequality  $> 0$  is replaced by  $\geq 0$ . For this reason we introduce a small positive constant  $\epsilon$  into the summation formulation for the non-penetration constraint.

$$\begin{aligned} & ((a_1 \geq -\epsilon/h) \wedge (a_2 \geq -\epsilon/h) \wedge (a_1 + a_2 \geq -\epsilon/h)) \vee \\ & ((a_1 \geq 0) \vee (a_2 \geq 0)) \\ \iff & \max\{-\epsilon/h, a_1\} + \max\{-\epsilon/h, a_2\} + \epsilon/h \geq 0. \end{aligned} \quad (24)$$

We divide  $\epsilon$  by the time step  $h$  so that  $\epsilon$  is proportional to distance instead of distance multiplied by time. The  $\epsilon/h$  value will create a small space that is mistakenly classified as in the valid region. In 2D the corner is “capped” by a plane that is perpendicular to the bisection of the two contact planes (see Fig. 4).

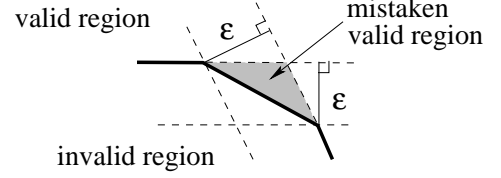


Fig. 4. The summation constraint mistakenly identifies a region with area proportional to  $\epsilon^2$  as valid.

**Proposition 2:** *The following LCP based on the summation formulation assures that the valid region is the union of two planes unioned with a “small” isosceles triangle at the corner of the invalid region. It also assures that no contact force is generated if there is no contact.*

Based on Eqn. (24) we enforce constraints on expressions  $a_1$  and  $a_2$ . As noted before both  $a_1$  and  $a_2$  represent expressions that use unknowns  $p_{1n}^{l+1}$  and  $p_{2n}^{l+1}$ . Artificial variables  $c_1$  and  $c_2$  are created. The summation formulation is given as follows:

$$0 \leq c_1 - a_1 - \epsilon/h \perp c_1 \geq 0 \quad (25)$$

$$0 \leq c_2 - a_2 - \epsilon/h \perp c_2 \geq 0 \quad (26)$$

$$0 \leq c_1 + c_2 - \epsilon/h \perp p_{1n}^{l+1} \geq 0 \quad (27)$$

$$0 \leq c_1 + c_2 - \epsilon/h \perp p_{2n}^{l+1} \geq 0. \quad (28)$$

Based on the the nonnegative and perpendicularity constraints in Eqns. (25) and (26) we have  $c_1 = \max\{-\epsilon/h, a_1\} + \epsilon/h$ . The inequality  $c_1 + c_2 - \epsilon/h \geq 0$  in Eqns. (27) and (28) will enforce the constraints in Eqn. (24) exactly.

We used an LCP solver to compute the unique frictionless solution  $z_a$  for the examples in Fig. 3(a). Many solutions are valid for the example shown in Fig. 3(b) and we present three of the many possible solutions. In both solutions  $\epsilon = 0.02$ , and  $\epsilon/h = 0.01$ .

In the example seen in Fig. 3(a) the solution  $z_a$  dictates that the point mass has velocity  $\mathbf{v}^{l+1} = [-3, 1]^T$  and position  $\mathbf{q}^{l+1} = [-2, 0]^T$  at the end of the current time step. If no contact occurs there is a unique solution that will match the solution given by the max formulation.

We used an LCP solver to compute  $z_{b1}$ , the first solution to the example in Fig. 3(b). In this solution the point mass makes contact with the horizontal plane but both planes contribute contact force. In this solution we have velocity  $\mathbf{v}^{l+1} = [-1.5, -0.5]^T$  and position  $\mathbf{q}^{l+1} = [-2, 0]^T$  at the end of the current time step. To illustrate the capped corner we produced  $z_{b2}$  by hand, the second solution to the example in Fig. 3(b). In this solution we have  $p_{1n}^{l+1} = 1.495$ ,  $p_{2n}^{l+1} = 0.495$ ,  $\mathbf{v}^{l+1} = [-0.505, -0.505]^T$  and position  $\mathbf{q}^{l+1} = [-0.001, -0.001]^T$ . Here we see a case where the point mass makes contact

with the capped corner and penetrates both the vertical and horizontal planes by half of  $\epsilon$ . For  $z_{b3}$ , the third solution to the example in Fig. 3(b), contact only occurs with the vertical plane but both planes contribute contact force. In this solution  $p_{1n}^{l+1} = 1.5$ ,  $p_{2n}^{l+1} = 0.13$ ,  $\nu^{l+1} = [-0.5, -1.87]^T$  and position  $q^{l+1} = [0, -2.7400]^T$ . We manually produced this solution to show that the small but arbitrary contact impulse  $p_{2n}^{l+1} = 0.13$  does produce a valid solution.

$$B_1 = B_2 = \begin{bmatrix} 1 & 0 & -1 & 0 \\ 0 & 1 & 0 & -1 \\ 1 & 1 & 0 & 0 \\ 1 & 1 & 0 & 0 \end{bmatrix}$$

$$b_1 = \begin{bmatrix} 1.49 \\ 0.49 \\ -0.01 \\ -0.01 \end{bmatrix} \quad b_2 = \begin{bmatrix} 1.49 \\ -0.51 \\ -0.01 \\ -0.01 \end{bmatrix}$$

$$\begin{bmatrix} c_1 \\ c_2 \\ p_{1n}^{l+1} \\ p_{2n}^{l+1} \end{bmatrix} \quad z_a = \begin{bmatrix} 0 \\ 0.51 \\ 0 \\ 0 \end{bmatrix}$$

$$z_{b1} = \begin{bmatrix} 0 \\ 0.01 \\ 0.5 \\ 0.5 \end{bmatrix} \quad z_{b2} = \begin{bmatrix} 0.005 \\ 0.005 \\ 1.495 \\ 0.495 \end{bmatrix} \quad z_{b3} = \begin{bmatrix} 0.01 \\ 0 \\ 1.5 \\ 0.13 \end{bmatrix}$$

As can be seen from example 1, this formulation does not constrain contact forces to only come from individual sides that are in contact. Rather, if any contact occurs then any normal force may be greater than 0, but if no contact occurs then no normal force may be greater than 0. This is not as accurate as the max formulation, and also leads to the existence of many possible solutions. When using the summation formulation for the first example, the point mass can lie anywhere on the horizontal plane between  $q^{l+1} = [-3, 0]^T$  and  $q^{l+1} = [-0.02, 0]^T$ , anywhere along the capped corner (diagonal  $y=-x$ ) between  $q^{l+1} = [-0.02, 0]^T$  and  $q^{l+1} = [0, -0.02]^T$ , or anywhere along the vertical plane between  $q^{l+1} = [0, -0.02]^T$  and  $q^{l+1} = [0, -1]^T$ . This corresponds to all possibilities where contact is made with at least one plane, penetration does not occur, and any combination of positive contact forces can be used.

The trade of accuracy for efficiency can be justified for certain classes of simulations. A nonconvex constraint is usually only necessary if a vertex-to-vertex collision is possible. If the vertex of a nonconvex constraint is close to a nearby face, then an intelligent physical simulation will not make a nonconvex constraint, but rather a single convex constraint that is parallel to the face (see Fig. 5). When a nonconvex constraint is truly necessary in the vertex-to-vertex case, contact from either of the planes will most likely appear plausible.

## VI. FRICTION AND MANY CONSTRAINTS

**Problem 2:** *Model the valid region in C-space as an arbitrary combination of unions and intersections for multiple planes and accurately calculate normal and friction forces.*

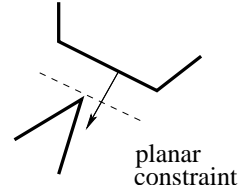


Fig. 5. In the vertex-to-face case the face of the upper object will define the contact plane and a simple convex planar constraint can be used.

**Proposition 3:** *Both the summation and max formulations can be generalized to an arbitrary set of planes. Once this is done friction calculations can be added easily.*

Using either the max or summation formulations, friction can be trivially added, since we have not changed the semantics of  $p_n^{l+1}$ . In our method, each element  $p_{in}^{l+1}$  represents the magnitude of the normal contact impulse just as in the usual convex formulation. For this reason the friction impulse vector  $p_f^{l+1}$  can friction scaling vector  $s^{l+1}$  can be calculated using  $\nu^{l+1}$  which depends on  $p_n^{l+1}$ . The definition for both of these vectors does not need to be changed from the Stewart-Trinkle formulation (Eqn. (5)).

When dealing with many constraints, we refer to a set of nonconvex constraints as a *group*. Furthermore, we refer to the planes within one group as the *sides* of the group. Two examples are given in Figs. 6(a) and 6(b).

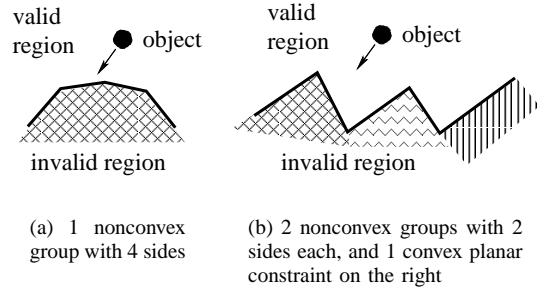


Fig. 6. Two examples of geometry that use nonconvex constraints.

In our previous examples, we showed the formulation for a single nonconvex group with two sides. Both of these formulations can be extended to many groups each with many sides. For the max constraint we have:

$$(a_1 \geq 0) \vee (a_2 \geq 0) \vee \dots \vee (a_n \geq 0) \quad (29)$$

$$\iff \max\{a_1, a_2, \dots, a_n\} \geq 0.$$

When using many sides the capped corner symptom of the summation formulation can be further exacerbated if the sides are very short (see Fig. 7). If extremely sharp corners and extremely short sides are avoided no nasty cases will be present and the capped corners will act exactly as they did for a nonconvex group with two sides. For the summation constraint we use the following relationship:

$$\max\{-\epsilon/h, a_1\} + \max\{-\epsilon/h, a_2\} + \dots + \max\{-\epsilon/h, a_n\} + (n-1)\epsilon/h \geq 0. \quad (30)$$

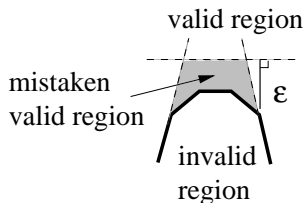


Fig. 7. The mistaken valid region can become larger when multiple close sides are grouped together using the summation formulation.

Variables from our earlier max and summation formulations that have a 1 or 2 subscript are specific to a side, and variables that do not have a subscript are specific to a group. The final matrix form for the LCP is given in the appendix at the end of this paper.

The number of linear constraints needed for modeling both convex and nonconvex constraints in C-space with friction is given below. The variables  $x$ ,  $y$  and  $g$  represent the number of convex constraints, the number of nonconvex sides, and the number of nonconvex groups respectively. The variable  $k$  represents the number of friction cone spanning vectors. The Stewart-Trinkle method can only model locally convex constraints in C-space.

form	number of constraints
max	$4y + 2g + x + (k + 1)(x + y)$
summation	$2y + x + (k + 1)(x + y)$
stewart	$x + (k + 1)(x)$

Multiple groups of nonconvex constraints, as well as convex planar constraints can all be included in the same LCP. However, it is important to note that it is only desirable to insert those constraints that may be active during the next time step. From the table above it is clear that modeling surfaces as convex half-planes requires less constraints. If geometry is locally convex in terms of the upcoming time step then it is more efficient to model the geometry using convex constraints.

## VII. IMPLEMENTATION

If either the max or summation formulations are used, care must be taken when choosing the value of  $\gamma$  and  $\epsilon$  respectively. Most LCP solvers do not test for symbolic equivalence to 0, but rather numeric equivalence within some small tolerance. If an extremely large value of  $\gamma$  or an extremely small value of  $\epsilon$  is used infeasible results may occur. This is because floating point operations on modern processors can lose large amounts of precision if the operands are of vastly different scale. This loss of precision can lead to non-physical results or an unsolvable LCP.

To make sure that roundoff error does not create an unsolvable LCP some LCP solvers will let you specify that the solution  $z$  may have elements that are slightly below 0. This is equivalent to allowing a small amount of interpenetration. Another option is to add small constants to the LCP so that contact forces may occur when objects are separated by only a miniscule distance. By incrementally increasing these

small tolerances the most accurate solution can be obtained. Assuring that there are no collinear normal vectors may also be important for finding a feasible solution [5].

Proximity detection is necessary to find which sides may come into contact in the upcoming time step. However, when using nonconvex constraints it may be necessary to include a side not because of potential contact, but rather because one nonconvex side effects another. In Fig. 8 the bottom side of the nonconvex corner will probably not come into contact with the object. However, if we do not include the bottom side the upper side will extend forever. Including the bottom side will, in effect, shorten the upper side.

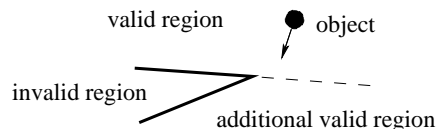


Fig. 8. The bottom side of the nonconvex group must be included in the LCP for the nonconvex constraint to be modeled properly.

## VIII. CONCLUSION

Using nonconvex constraints it is now possible to represent any 2D polygonal object using the LCP formulation. All 2D polygons can be triangulated and every triangle can be represented by 3 nonconvex constraints, (the interior of any triangle is convex, but the exterior is nonconvex). Not all general polytopes can be triangulated, but all polytopes can be decomposed into simplices. A simplex is always internally convex, and its exterior can be represented as a combination of nonconvex hyper-plane constraints. Using our method it is now possible to represent any simple polytope using linear complementarity.

While the nonconvex constraints proposed here follow most physical properties maintained by the convex constraints, there is an element of nondeterminism in the nonconvex formulation. Since the interpenetration constraint for a nonconvex group can be satisfied by any one or more of the many sides, the LCP solver has a fair amount of leeway in choosing how to deal with interpenetrating objects. Furthermore, in the summation case contact force is not restricted to come from planes that are in contact. This means that when using the summation formulation the final normal force may lie anywhere within the cone constructed by the normals at each nonconvex side. These issues are shown in Fig. 9(a) and 9(b).

## ACKNOWLEDGMENTS

The authors wish to thank Jong-Shi Pang and Liu Guanfeng for their technical guidance and suggestions. The authors were partially supported by NSF grant #0139701.

## REFERENCES

- [1] P. Lötstedt, "Coulomb friction in two-dimensional rigid-body systems," *Zeitschrift für Angewandte Mathematik und Mechanik*, vol. 61, pp. 605–615, 1981.

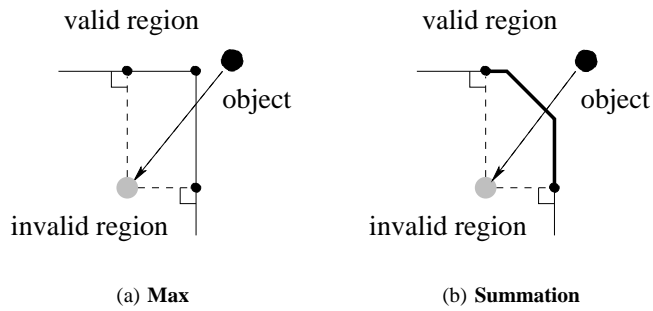


Fig. 9. Without an applied normal force the point mass will penetrate the corner. Bold dots and bold lines indicate possible final positions for the point mass. There are three possible solutions when using the max formulation, and a range of solutions when using the summation formulation. The pictures depict the frictionless case.

[2] D. Baraff, "Issues in computing contact forces for non-penetrating rigid bodies," *Algorithmica*, pp. 292–352, Oct. 1993.

[3] F. Pfeiffer and C. Glocker, *Multibody Dynamics with Unilateral Contacts*. Wiley, 1996.

[4] D. Baraff, "Curved surfaces and coherence for non-penetrating rigid body simulation," *Computer Graphics*, vol. 24, no. 4, pp. 19–28, 1990. [Online]. Available: [citeseer.nj.nec.com/baraff90curved.html](http://citeseer.nj.nec.com/baraff90curved.html)

[5] D. Stewart and J. Trinkle, "An implicit time-stepping scheme for rigid body dynamics with inelastic collisions and coulomb friction," *International Journal of Numerical Methods in Engineering*, vol. 39, pp. 2673–2691, 1996.

[6] R. W. Cottle, J. Pang, and R. E. Stone, *The Linear Complementarity Problem*. Academic Press, 1992.

## APPENDIX

In this appendix we detail the final form of the LCP for nonconvex constraints using the max and summation formulations. Both formulations can represent convex and nonconvex constraints, and both formulations use a frictional contact model. We assume here that the constraints are sorted so that the first  $y$  constraints are nonconvex, and the next  $x$  constraints are convex. The number of nonconvex groups is represented as  $g$ . The vector  $e_n$  is defined as  $e_n = [1, 1, \dots, 1]^T \in \mathbb{R}^n$ . The matrix  $E$  retains the same definition from our original dynamics formulation in Eqn. (5). The matrix  $I_n \in \mathbb{R}^{n \times n}$  is defined as the square identity matrix of size  $n$ . The selection matrix  $D \in \mathbb{R}^{g \times y}$  identifies whether a nonconvex side is a member of a specific nonconvex group. Each element  $d_{ij}$  at row  $i$  and column  $j$  in  $D$  has value 1 if nonconvex group

$i$  contains nonconvex side  $j$ , and 0 otherwise. The value  $D^T D$  is a square matrix such that  $dd_{ij}$  is 1 if side  $i$  and side  $j$  are in the same group, and 0 otherwise. The value  $D^T D e_y$  is a vector such that  $dde_i$  is equal to the size of the group containing side  $i$ . The unknown  $p_n^{l+1}$  and the vector  $f^l$  are both split in two components, where one component has the first  $y$  rows (denoted with a subscript  $y$ ), and the other component has the last  $x$  rows (denoted with a subscript  $x$ ). The matrices  $W_n$  and  $U$ , are also split into two components, where one component has the first  $y$  columns and the other component has the last  $x$  columns. These new components  $p_x^{l+1}$ ,  $p_y^{l+1}$ ,  $f_x^l$ ,  $f_y^l$ ,  $W_x$ ,  $W_y$ ,  $U_x$  and  $U_y$  are all listed in Eqn. (31).

$$p_n^{l+1} = \begin{bmatrix} p_y^{l+1} \\ p_x^{l+1} \end{bmatrix} \quad f^l = \begin{bmatrix} f_y^l \\ f_x^l \end{bmatrix} \quad W_n = [W_y \quad W_x] \quad U = [U_y \quad U_x] \quad (31)$$

$$B_{max} = \begin{bmatrix} I_y & 0 & 0 & 0 & 0 & W_y^T M^{-1} W_y & W_y^T M^{-1} W_x & W_y^T M^{-1} W_f & 0 \\ 0 & 0 & D & 0 & 0 & 0 & 0 & 0 & 0 \\ I_y & D^T & 0 & 0 & 0 & 0 & 0 & 0 & 0 \\ 0 & 0 & 0 & I_y & 0 & W_y^T M^{-1} W_y & W_y^T M^{-1} W_x & W_y^T M^{-1} W_f & 0 \\ 0 & I_g & 0 & 0 & 0 & 0 & 0 & 0 & 0 \\ 0 & D^T & 0 & I_y & 0 & 0 & 0 & 0 & 0 \\ 0 & 0 & 0 & 0 & 0 & W_x^T M^{-1} W_y & W_x^T M^{-1} W_x & W_x^T M^{-1} W_f & 0 \\ 0 & 0 & 0 & 0 & 0 & W_f^T M^{-1} W_y & W_f^T M^{-1} W_x & W_f^T M^{-1} W_f & E \\ 0 & 0 & 0 & 0 & 0 & U_y & U_x & -E^T & 0 \end{bmatrix} \quad (32)$$

$$b_{max} = \begin{bmatrix} W_y^T (\nu^l + M^{-1} p_{ext}) + f_y^l/h - e_y \\ -e_g \\ -\gamma e_y \\ W_y^T (\nu^l + M^{-1} p_{ext}) + f_y^l/h \\ (-\gamma + 1)e_g \\ (-\gamma + 1)e_y \\ W_x^T (\nu^l + M^{-1} p_{ext}) + f_x^l/h \\ W_f^T (\nu^l + M^{-1} p_{ext}) \\ 0 \end{bmatrix} \quad z_{max} = \begin{bmatrix} c \\ d \\ g \\ h \\ p \\ p_y^{l+1} \\ p_x^{l+1} \\ p_f^{l+1} \\ s^{l+1} \end{bmatrix} \quad (33)$$

$$B_{sum} = \begin{bmatrix} I_y & -W_y^T M^{-1} W_y & -W_y^T M^{-1} W_x & -W_y^T M^{-1} W_f & 0 \\ D^T D & 0 & 0 & 0 & 0 \\ 0 & W_x^T M^{-1} W_y & W_x^T M^{-1} W_x & W_x^T M^{-1} W_f & 0 \\ 0 & W_f^T M^{-1} W_y & W_f^T M^{-1} W_x & W_f^T M^{-1} W_f & E \\ 0 & U_y & U_x & -E^T & 0 \end{bmatrix} \quad (34)$$

$$b_{sum} = \begin{bmatrix} -W_y^T (\nu^l + M^{-1} p_{ext}) - f_y^l/h - (\epsilon/h)e_y \\ -(\epsilon/h)(D^T D e_y - e_y) \\ W_x^T (\nu^l + M^{-1} p_{ext}) + f_x^l/h \\ W_f^T (\nu^l + M^{-1} p_{ext}) \\ 0 \end{bmatrix} \quad z_{sum} = \begin{bmatrix} c \\ p_y^{l+1} \\ p_x^{l+1} \\ p_f^{l+1} \\ s^{l+1} \end{bmatrix} \quad (35)$$